determines pollen specificity in self-incompatibility interactions has important implications for how S-RNases specifically inhibit the growth of self-pollen tubes. It has been shown that RNase activity is required for the function of S-RNases[16], and that both self and non-self S-RNases are taken up by pollen tubes growing in a pistil[17]. Therefore, it seems that only self S-RNase is able to function inside a pollen tube, degrading RNA substrate(s) to inhibit pollen-tube growth. This raises the question as to how the toxicity of non-self S-RNases is neutralized.

Recently, it has been shown that an *S*-locus F-box protein of *Antirrhinum* (Scrophulariaceae), AhSLF-S_2, is a likely component of the SCF complex (composed of Skp1, Cullin1, Rbx1 and an F-box protein)[18], which is involved in ubiquitin-mediated protein degradation by the 26S proteasome[19]. Interestingly, AhSLF-S_2 interacts with both self and non-self S-RNases, but appears to mediate degradation of only non-self S-RNases[18]. Because there are multiple *S*-linked F-box genes in *Antirrhinum*[8] and *P. inflata*[14], whether *AhSLF* is an orthologue of *PiSLF* remains to be determined. If PiSLF is a component of the SCF complex, its interaction with a domain common to all S-RNases might lead to ubiquitination and degradation, but this interaction would be prevented by an alternate specific interaction between PiSLF and its cognate self S-RNase. □

Methods

DNA and RNA gel blot analyses

Isolation of genomic DNA from young leaves and genomic DNA blot analysis were carried out as previously described[14], as was isolation of total RNA and RNA gel blot analysis[20].

Construction of transgene and *Agrobacterium*-mediated transformation

An ~11-kb DNA fragment containing *PiSLF*$_2$ was released from BAC clone 145J16 (ref. 12) by *Bam*HI digestion and cloned into the *Bam*HI site of pBluescript KS + (Stratagene) to yield pBS-11K. pBS-11K was digested with *Sal*I, made blunt-ended by Klenow enzyme, and digested with *Xba*I to release a ~ 4.3-kb fragment containing *PiSLF*$_2$. A Ti plasmid, pBI101 (Clontech), was digested with *Sac*I, made blunt-ended by T4 DNA polymerase, and digested with *Xba*I. The ~4.3-kb DNA fragment containing *PiSLF*$_2$ was ligated into the *Xba*I site and the blunt-end site of pBI101 (see Supplementary Fig. S2). The recombinant Ti plasmid was electroporated into *Agrobacterium tumefaciens* strain LBA4404 using a Cell-Porator (Life Technologies). The transformation of *P. inflata* leaf strips with *Agrobacterium* was carried out as described previously[2].

PCR and RT–PCR

To clone *PiSLF*$_1$, *PiSLF*$_2$ and *PiSLF*$_3$ by RT–PCR, cDNA was separately synthesized from 5 μg of total RNA isolated from S_1, S_2 and S_3 pollen using 200 units of SuperScript II RNaseH-reverse transcriptase (Invitrogen). PCR was carried out on the cDNA of each *S*-genotype in a standard reaction buffer containing 0.25 μM each of forward primer (5′-GATCCAGTTGAATGAGATGG-3′) and reverse primer, oligo $(dT)_{17}$, and two units of Taq DNA polymerase (Fisher Scientific). The reaction mixture was denatured at 94 °C for 1 min, then subjected to 30 cycles, with each cycle consisting of denaturation at 94 °C for 45 s, annealing at 45 °C for 45 s and extension at 72 °C for 1 min. After the last cycle, the sample was kept at 72 °C for an additional 10 min. PCR products were gel-purified and ligated into pGEM-T Easy vector (Promega).

To assess the presence of the *PiSLF*$_2$ transgene in T_0 and T_1 transgenic plants, PCR was carried out on 5 ng of genomic DNA isolated from each plant as described above, except that the forward primer was 5′-TATTAACATTTCCAGTGAAATCTCTTAT-3′, the reverse primer was 5′-GTATCAGGCATTTTCATATCATGAAAC-3′ and the annealing temperature was 58 °C. To examine the expression of *PiSLF*$_1$ and *PiSLF*$_2$ in T_0 transgenic plants, cDNA was synthesized as described above. PCR conditions were the same as those described above except that for *PiSLF*$_1$, the annealing temperature was 63 °C and the primers used were: 5′-TGTTAACATTTCCCGTTAAATCTCTCCT-3′ (forward primer) and 5′-ATCTTTT ACTGGATCAATAGAGCTTATTGG-3′ (reverse primer). To use actin as the control in RT–PCR, two primers, 5′-GGCATCACACTTTCTACAATGAGC-3′ (forward) and 5′-GATATCCACATCACATTTCATGAT-3′ (reverse), were designed on the basis of the sequence of pollen-expressed *Arabidopsis* actin 12 (At3g46520).

Received 17 December 2003; accepted 30 March 2004; doi:10.1038/nature02523.

1. de Nettancourt, D. *Incompatibility and Incongruity in Wild and Cultivated Plants* (Springer, Berlin, 2001).
2. Lee, H.-S., Huang, S. & Kao, T.-h. S proteins control rejection of incompatible pollen in *Petunia inflata*. *Nature* **367,** 560–563 (1994).
3. Murfett, J., Atherton, T. L., Mou, B., Gasser, C. S. & McClure, B. A. *S-RNase* expressed in transgenic *Nicotiana* causes *S*-allele-specific pollen rejection. *Nature* **367,** 563–566 (1994).
4. Kao, T.-h. & Tsukamoto, T. The molecular and genetic bases of S-RNase-based self-incompatibility. *Plant Cell* advance online publication 9 March 2004 (doi:10.1105/tpc.016154).
5. Lai, Z. *et al.* An F-box gene linked to the self-incompatibility (*S*) locus of *Antirrhinum* is expressed specifically in pollen and tapetum. *Plant Mol. Biol.* **50,** 29–42 (2002).
6. Entani, T. *et al.* Comparative analysis of the self-incompatibility (*S*-) locus region of *Prunus mume*: identification of a pollen-expressed F-box gene with allelic diversity. *Genes Cells* **8,** 203–213 (2003).
7. Ushijima, K. *et al.* Structural and transcriptional analysis of the self-incompatibility locus of almond: identification of a pollen-expressed F-box gene with haplotype-specific polymorphism. *Plant Cell* **15,** 771–781 (2003).
8. Zhou, J. *et al.* Structural and transcriptional analysis of *S*-locus F-box (*SLF*) genes in *Antirrhinum*. *Sex. Plant Reprod.* **16,** 165–177 (2003).
9. Golz, J. F., Su, V., Clarke, A. E. & Newbigin, E. A molecular description of mutations affecting the pollen component of the *Nicotiana alata S* locus. *Genetics* **152,** 1123–1135 (1999).
10. Golz, J. F., Oh, H.-Y., Su, V., Kusaba, M. & Newbigin, E. Genetic analysis of *Nicotiana* pollen-part mutants is consistent with the presence of an S-ribonuclease inhibitor at the *S* locus. *Proc. Natl Acad. Sci. USA* **98,** 15372–15376 (2001).
11. McCubbin, A. G., Zuniga, C. & Kao, T.-h. Construction of a binary artificial chromosome library of *Petunia inflata* and the identification of large genomic fragments linked to the self-incompatibility (*S*-) locus. *Genome* **43,** 820–826 (2000).
12. Wang, Y. *et al.* Chromosome walking in the *Petunia inflata* self-incompatibility (*S*-) locus and gene identification in an 881-kb contig containing S_2-*RNase*. *Plant Mol. Biol* (in the press).
13. Ai, Y. *et al.* Self-incompatibility in *Petunia inflata*: isolation and characterization of cDNAs encoding three *S*-allele-associated proteins. *Sex. Plant Reprod.* **3,** 130–138 (1990).
14. Wang, Y., Wang, X., McCubbin, A. G. & Kao, T.-h. Genetic mapping and molecular characterization of the self-incompatibility (*S*-) locus in *Petunia inflata*. *Plant Mol. Biol.* **53,** 565–580 (2003).
15. Luu, D.-T. *et al.* Rejection of *S*-heteroallelic pollen by a dual-specific S-RNase in *Solanum chacoense* predicts a multimeric self-incompatibility pollen component. *Genetics* **159,** 329–335 (2001).
16. Huang, S., Lee, H.-S., Karunanandaa, B. & Kao, T.-h. Ribonuclease activity of *Petunia inflata* S proteins is essential for rejection of self-pollen. *Plant Cell* **6,** 1021–1028 (1994).
17. Luu, D.-T., Qin, K., Morse, D. & Cappadocia, M. S-RNase uptake by compatible pollen tubes in gametophytic self-incompatibility. *Nature* **407,** 649–651 (2000).
18. Qiao, H. *et al.* The F-box protein AhSLF-S_2 physically interacts with S-RNases that may be inhibited by the ubiquitin/26S proteasome pathway of protein degradation during compatible pollination in *Antirrhinum*. *Plant Cell* **16,** 582–595 (2004).
19. Bai, C. *et al.* Skp1 connects cell cycle regulation to the ubiquitin proteolysis machinery through a novel motif, the F-box. *Cell* **86,** 263–274 (1996).
20. Skirpan, A. L. *et al.* Isolation and characterization of kinase interacting protein 1, a pollen protein that interacts with the kinase domain of PRK1, a receptor-like kinase of petunia. *Plant Physiol.* **126,** 1480–1492 (2001).
21. Mu, J.-H., Lee, H.-S. & Kao, T.-h Characterization of a pollen-expressed receptor-like kinase gene of *Petunia inflata* and the activity of its encoded kinase. *Plant Cell* **6,** 709–721 (1994).

Supplementary Information accompanies the paper on **www.nature.com/nature**.

Acknowledgements We thank A. H. Omeis for the greenhouse work, J. Wang for routine laboratory assistance and the Monsanto Sequencing Facility for sequencing the BAC clones. This work was supported by a Predoctoral Fellowship for Students with Disabilities from the National Institutes of Health (P.E.D.) and by grants from the National Science Foundation (T.-h.K.).

Competing interests statement The authors declare that they have no competing financial interests.

Correspondence and requests for materials should be addressed to T.-h.K. (txk3@psu.edu).

Self-incompatibility triggers programmed cell death in *Papaver* pollen

Steven G. Thomas & Vernonica E. Franklin-Tong

School of Biosciences, University of Birmingham, Edgbaston, Birmingham B15 2TT, UK

Sexual reproduction in many angiosperm plants involves self-incompatibility (SI), which is one of the most important mechanisms to prevent inbreeding. SI is genetically controlled by the *S*-locus, and involves highly specific interactions during pollination between pollen and the pistil on which it lands. This results in the rejection of incompatible ('self') pollen, whereas compatible ('non-self') pollen is allowed to fertilize the plant[1]. In *Papaver rhoeas*, S-proteins encoded by the stigma component of the *S*-locus interact with incompatible pollen, triggering a Ca^{2+}-dependent signalling network[2–7], resulting in the inhibition of pollen-tube growth. Programmed cell death (PCD) is a

Table 1 **Alleviation of SI-induced DNA fragmentation and tube-growth inhibition by DEVD**

Treatment	DNA fragmentation (%)		Mean pollen-tube length (μm)	
	Incompatible pollen	Compatible pollen	Incompatible pollen	Compatible pollen
Control (untreated)	3.33 ± 1.76	4.00 ± 1.15	536.3 ± 78.9	546.7 ± 80.2
SI	71.58 ± 2.24	2.83 ± 0.60	162.9 ± 5.9	520.7 ± 78.6
SI + DEVD	18.97 ± 5.53	2.00 ± 0.00	376.0 ± 40.2	490.9 ± 27.8
SI + YVAD	52.00 ± 5.29	6.38 ± 3.43	160.8 ± 5.6	532.5 ± 73.6

SI, SI induction; SI + DEVD, DEVD treatment before SI induction; SI + YVAD, YVAD treatment before SI induction. Results are means ± s.e.m.; $n = 3$ in all cases.

mechanism used by many organisms to destroy unwanted cells in a precisely regulated manner[8–10]. Here we show that PCD is triggered by SI in an *S*-specific manner in incompatible pollen. This provides a demonstration of a SI system using PCD, revealing a novel mechanism to prevent self-fertilization. Furthermore, our data reveal that the response is biphasic; rapid inhibition of pollen-tube growth is followed by PCD, which is involved in a later 'decision-making' phase, making inhibition irreversible.

Programmed cell death (PCD) has several key diagnostic features. These include nuclear DNA fragmentation, leakage of cytochrome *c* from the mitochondria into the cytosol, and cleavage of poly(ADP-ribose) polymerase (PARP)[8,11,12]. A key enzyme involved in apoptosis in animal cells is caspase-3, which is activated in an autoprocessing cascade[13] and is instrumental in the cleavage of nuclear DNA and PARP[14,15]. Although it is generally accepted that apoptosis does not occur in plant cells, PCD in plants shares some apoptotic features. The tetrapeptide DEVD is an inhibitor of caspase-3 and has been used to provide evidence for a caspase-like activity in apoptotic animal cells and in plant cells undergoing PCD[16–18]. We have used these markers and tools to investigate whether PCD is triggered in incompatible pollen as a consequence of the SI response.

We have demonstrated previously that DNA fragmentation is stimulated during SI in an *S*-specific manner[7]. Although our results indicated that PCD might be triggered in incompatible pollen, they were not conclusive. Here we present data demonstrating that DNA fragmentation was inhibited by pretreatment with the caspase-3 inhibitor I peptide, Ac-DEVD-CHO (DEVD). In incompatible pollen tubes that had been SI induced, a significantly increased incidence of DNA fragmentation, 21.5-fold that of untreated pollen, was observed (Table 1, $P < 0.001$). The same treatment of compatible pollen tubes revealed a highly significant difference in the DNA fragmentation compared with incompatible pollen tubes ($P < 0.001$), thereby demonstrating *S*-specificity. When DEVD was included before the SI treatment of incompatible pollen tubes, DNA fragmentation was significantly decreased in comparison with that induced by SI alone (Table 1, $P < 0.001$), and the DNA fragmentation was not significantly different from that found in untreated pollen tubes ($P = 0.054$ (n.s.)). We also used the caspase-1 inhibitor 1 peptide, Ac-YVAD-CHO (YVAD), as a potential negative control. Although less DNA fragmentation was detected in SI-induced incompatible pollen tubes pretreated with YVAD (Table 1), the effect of YVAD on the SI response was considerably less than that of DEVD ($P = 0.027$) and pollen tubes still exhibited 52.0% DNA fragmentation. Together, these data provide evidence that a DEVDase/caspase-like activity is triggered in an *S*-specific manner in incompatible pollen by the SI response, and that this mediates DNA fragmentation. Although the *Arabidopsis* genome sequence reveals no caspase homologues, reports of caspase-like activities in plant cells with sensitivity to animal caspase-3 inhibitors[18,19] implicate their involvement in PCD.

We also examined the effects of these treatments on pollen-tube inhibition (Table 1, Fig. 1). Incompatible SI-induced pollen tubes were significantly shorter than compatible pollen tubes (Table 1; $P = 0.01$), which achieved the same length as the untreated incompatible pollen tubes (Table 1; $P = 0.896$ (n.s.)). Pretreatment with DEVD markedly alleviated the pollen-tube inhibition stimulated by SI in incompatible pollen (Table 1; $P = 0.006$). However, pretreatment with YVAD had no significant effect on SI-induced pollen-tube inhibition (Table 1, $P = 0.802$ (n.s.)), and tube lengths were almost identical to those treated with S-proteins alone. These data therefore provide good evidence that a DEVDase/caspase-like activity is involved in SI-mediated pollen-tube inhibition.

As it is well established that SI arrests pollen-tube growth rapidly[2,5], the data also indicated that pollen-tube growth might be able to recommence, with the implication that DEVDase activity can be triggered after initial arrest. Monitoring growth rates confirmed this idea (Fig. 1). Pollen-tube growth arrested within 5 min of SI induction (Fig. 1a); pretreatments with DEVD and YVAD had no effect on growth rate (Fig. 1b). Pretreatment of incompatible pollen tubes with DEVD allowed growth after SI (Fig. 1c), whereas YVAD showed no alleviation of SI-induced inhibition. The DEVD–SI response was quite variable, but examination of individual pollen tubes (Fig. 1d) revealed that arrest occurred for between 15 and 45 min, after which pollen-tube growth reinitiated. Detailed examination of DEVD-treated pollen

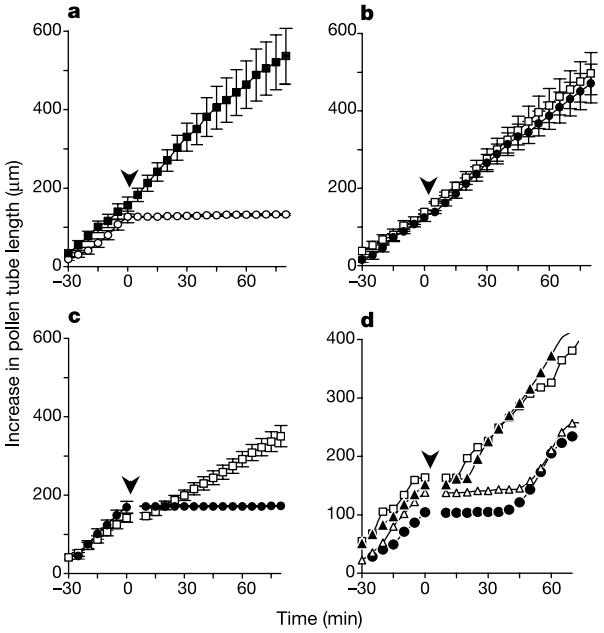

Figure 1 DEVD permits pollen-tube growth recovery after arrest by SI. **a**, SI induction (arrow) after pretreatment with GM (circles; $n = 7$) rapidly inhibited growth. Addition of GM instead of incompatible S proteins (squares; $n = 8$) at the arrow had no effect. Results are means ± s.e.m. **b**, Pretreatment of control pollen tubes with DEVD (squares; $n = 6$) or YVAD (circles; $n = 5$) before the addition of GM (arrow) had no effect on pollen-tube growth. Results are means ± s.e.m. **c**, Pollen tubes pretreated with DEVD followed by SI induction (squares; $n = 16$) grew after SI. Pretreatment with YVAD (circles; $n = 7$) before SI had no effect on inhibition. Arrow indicates SI induction. Results are means ± s.e.m. **d**, The growth of individual pollen tubes (represented by different symbols) responding to DEVD + SI was inhibited for between 15 and 45 min after SI; growth then recovered. The arrow indicates SI induction.

tubes between 0 and 10 min after SI revealed no growth during this period ($n = 19$; data not shown). Because YVAD, unlike DEVD, did not result in any significant pollen tube recovery, this supports the idea that it is the specific DEVD sequence that has this effect. Together, these data suggest not only that a DEVDase/caspase-like activity is activated by the SI response, but that it also has a crucial function in the inhibition of incompatible pollen-tube growth. Thus, there seems to be a biphasic SI response: rapid inhibition of pollen-tube growth, followed later by DEVDase activation, which presumably makes inhibition irreversible.

Cytochrome *c* leakage into the cytosol is a classic marker for PCD in many organisms, including plants[20,21]. Here we present evidence that cytochrome *c* release from the mitochondria into the cytosol was stimulated by SI induction in incompatible pollen tubes (Fig. 2a). An increase in cytochrome *c* concentration was detected in cytosolic extracts from incompatible pollen 120 min after SI induction when compared with concentrations in compatible pollen tubes at the same time point (Fig. 2a); this demonstrates the *S*-specificity of this response. These data provide additional evidence that PCD is triggered in incompatible pollen during SI.

We investigated the timing of cytochrome *c* release into the cytosol, because this might give an indication of how early PCD is triggered in incompatible pollen (Fig. 2b). Small but detectable amounts of cytochrome *c* in incompatible pollen were observed as early as 10 min after SI induction. The concentration of cytosolic cytochrome *c* increased further, and by 120 min after SI induction, amounts in the cytosol of incompatible pollen tubes were significantly higher than those in compatible pollen tubes at the same time point (Fig. 2b; $P = 0.001$). Controls consistently showed no sign of cytochrome *c* in the cytosol.

The cytosolic concentration of free Ca^{2+} ($[Ca^{2+}]_i$) acts as a second messenger in the SI response in *Papaver*[2]. We investigated whether increases in $[Ca^{2+}]_i$ might also stimulate cytochrome *c* leakage. Mastoparan has been used previously to stimulate increases in $[Ca^{2+}]_i$ in *Papaver* pollen tubes[22]. Here we show that mastoparan stimulates the release of cytochrome *c* into the cytosol. A significant increase in cytosolic cytochrome *c*, from zero to $(9.92 \pm 1.4) \times 10^4$ counts mm^{-2} ($n = 3$, $P = 0.002$) was observed after 5 min of treatment with mastoparan. This indicates increases in $[Ca^{2+}]_i$ upstream of cytochrome *c* release, thereby providing a possible link with SI signalling.

PARP is a classic substrate for caspase-3 activity in animal cells and is often used as evidence for PCD. At least two PARP genes are known to be present in plants[23,24], so PARP could be a substrate for this activity. We examined SI-induced pollen protein extracts for a caspase-like cleavage activity *in vitro*, using bovine PARP as a substrate, and show that incompatible pollen extracts contain such an activity (Fig. 3a). A 24-kDa PARP cleavage fragment was consistently detected only in PARP samples incubated with incompatible SI-induced pollen extracts ($n = 8$). This, coupled with a

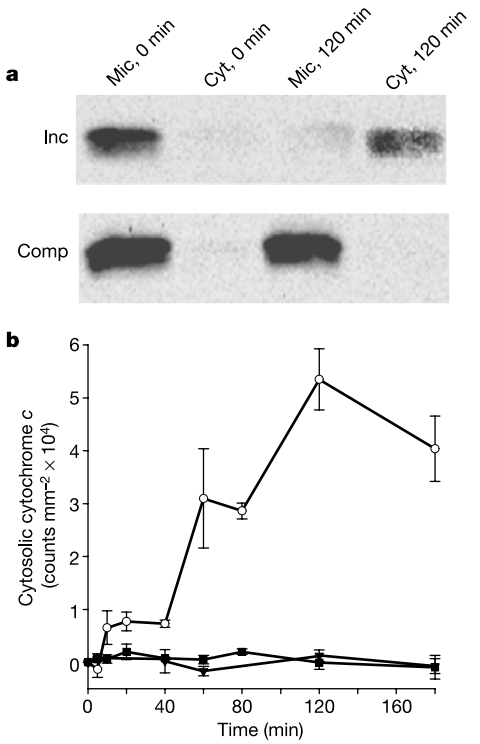

Figure 2 SI triggers the release of cytochrome *c* into the cytosol of incompatible pollen tubes. **a**, Microsomal (Mic) and cytosolic (Cyt) protein extracts from incompatible (Inc) and compatible (Comp) pollen that had undergone SI were examined for the presence of cytochrome *c* by using western blotting. Cytochrome *c* was present in microsomal, but not cytosolic, fractions from both compatible and incompatible pollen tubes at zero time. Increased amounts of cytochrome *c* were detected in the cytosolic fraction from incompatible pollen tubes 120 min after SI induction (lane 4, top panel), whereas compatible pollen tubes at the same time point showed no such increase (lane 4, bottom panel). **b**, After SI induction, the amount of cytosolic cytochrome *c* in incompatible (circles) pollen tubes increased over time. Compatible (triangles) and untreated (squares) pollen showed no change. Data are cytochrome *c* amounts (mean ± s.e.m.; $n = 3$) ascertained by quantification from western blots.

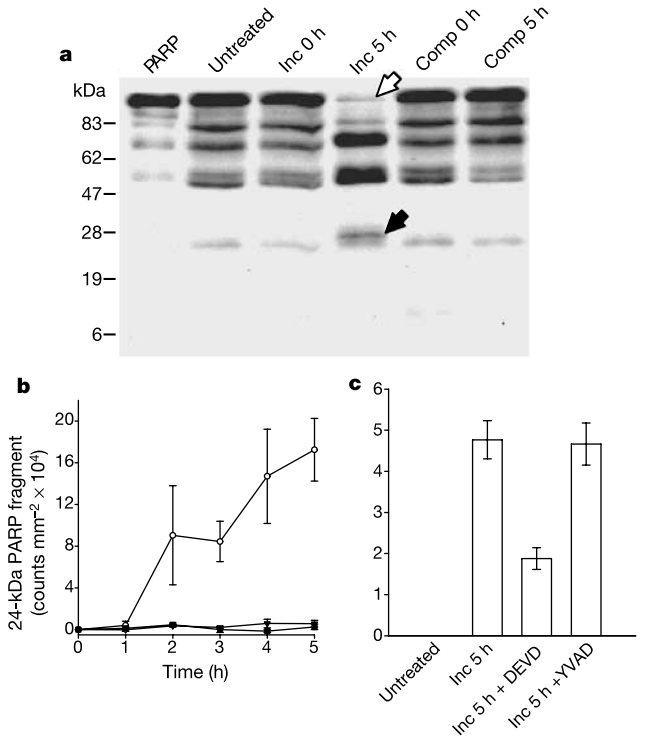

Figure 3 SI-stimulated incompatible pollen has an activity that can cleave bovine PARP. **a**, A PARP 24-kDa cleavage fragment (filled arrowhead) was detected in samples incubated with incompatible pollen extracts that had undergone SI for 5 h (Inc 5 h). A decrease in the full-length PARP protein (open arrow) was also evident. The PARP cleavage fragment was not detected in samples of PARP incubated without extracts (PARP) or with untreated, compatible (Comp) or incompatible (Inc) pollen extracts at zero time. **b**, PARP-cleavage activity in SI-induced incompatible (circles) pollen extracts increased in relation to the length of time after SI. Compatible (triangles) and untreated (squares) pollen extracts showed no PARP-cleavage activity. Results are amounts of 24-kDa PARP cleavage fragment (mean ± s.e.m.; $n = 3$) measured by quantification from western blots. **c**, Pretreatment of SI-induced pollen-tube extracts with DEVD (Inc 5 h + DEVD) decreased the amount of 24-kDa PARP cleavage fragment, whereas YVAD (Inc 5 h + YVAD) did not. Inc 5 h, SI-induced pollen-tube extracts.

corresponding decrease in the amount of uncleaved PARP (116 kDa) provides compelling evidence that a PARP-cleavage activity is triggered by SI. The *S*-specificity of this PARP-cleavage activity was demonstrated because neither compatible pollen that had been SI treated nor untreated pollen extracts generated a detectable 24-kDa PARP fragment (Fig. 3a). Investigation of the temporal activation of PARP-cleavage activity in incompatible pollen tubes by SI (Fig. 3b) revealed that the 24-kDa fragment was first detected 2 h after SI induction and it increased over time: 5 h after SI induction it was significantly higher than at zero time (Fig. 3b; $P = 0.005$). Because PARP is involved in nuclear DNA repair[25], the timing of detectable PARP-cleavage activity in incompatible pollen, which occurs before the detection of DNA fragmentation, is plausible.

We used mastoparan and La^{3+} to investigate whether Ca^{2+} might be implicated in stimulating PARP-cleavage activity in pollen tubes. Mastoparan stimulated a PARP-cleavage activity in pollen tubes, resulting in a highly significant increase in the abundance of the PARP 24-kDa cleavage product, $(2.88 \pm 0.366) \times 10^5$ counts mm^{-2} compared with zero in the untreated controls ($n = 4$, $P < 0.001$). We used La^{3+}, which blocks SI-stimulated Ca^{2+} influx in *Papaver* pollen tubes[26], to see whether this might provide further evidence for an involvement of Ca^{2+}. A comparison between the PARP-cleavage activity induced by SI in incompatible pollen tubes and the same treatment incubated with La^{3+} before SI induction resulted in a significant decrease ($70 \pm 7.7\%$, $n = 3$, $P = 0.002$) in the 24-kDa PARP fragment. Together these data indicate that increases in $[Ca^{2+}]_i$ in pollen can trigger PARP-cleavage activity, thereby providing a tangible link to Ca^{2+} signalling stimulated by SI.

We investigated whether the PARP-cleavage activity in incompatible pollen extracts might be due to a caspase-like activity by using DEVD as a competitive inhibitor and YVAD as a negative control (Fig. 3c). Pretreatment of SI-induced incompatible pollen extracts with DEVD before incubation with bovine PARP significantly decreased the amount of PARP 24-kDa cleavage product, a $60.38 \pm 5.66\%$ decrease ($n = 3$, $P < 0.001$) compared with that found in the same extracts in the absence of DEVD. The equivalent comparison with YVAD pretreatment gave a $0.64 \pm 14.23\%$ decrease ($n = 3$, $P = 0.966$). This clearly indicates the involvement of a DEVDase/caspase-like activity induced by SI in the generation of the 24-kDa PARP cleavage fragment.

In conclusion, we have examined the SI response in pollen of *P. rhoeas* for several diagnostic features of PCD. Together, our data provide compelling evidence that PCD is triggered by SI in an *S*-specific manner in incompatible pollen. The use of DEVD provides evidence for the involvement of a caspase-like activity in making the inhibition of incompatible pollen tube growth irreversible. The demonstration of PCD as a novel mechanism for the prevention of self-fertilization, together with evidence for a biphasic response, provides a significant advance in our understanding of SI and the regulation of pollen-tube growth. Because this SI system uses similar mechanisms to those used by the hypersensitive response in plant–pathogen interactions[17], it provides evidence supporting previous speculative links between these recognition systems[27,28]. □

Methods

SI induction and DNA fragmentation

Pollen was grown at 25 °C for 1 h on solid germination medium (GM)[5] before SI induction, which was achieved by the addition of recombinant stigmatic S proteins S_1e and S_8e to S_1S_8 (incompatible) and S_2S_6 (compatible) pollen[29]; pollen was incubated for a further 8 h. To test the effect of caspase inhibitors on SI-induced DNA fragmentation, pollen was grown for 1 h in the presence of 100 μM Ac-DEVD-CHO or Ac-YVAD-CHO (Biomol) before SI induction and incubation for 8 h. For 'untreated' controls, pollen was grown for 1 h, an aliquot of liquid GM (ref. 3) added, and pollen was incubated for a further 8 h. Times indicated are after SI induction. Pollen tubes were then fixed in 4% paraformaldehyde[7] and labelled with a Deadend fluorimetric TUNEL kit (Promega). Pollen tubes were scored for DNA fragmentation (50 tubes per treatment; $n = 3$) with a Nikon T300 fluorescence microscope. Capture and analysis of images was achieved with a Quips PathVysion image analysis system (Applied Imaging International Ltd).

For the measurement of absolute pollen-tube lengths, pollen was treated as above but was incubated at 25 °C for 2 h, fixed in 4% paraformaldehyde and mounted in Tris-buffered saline (pH 7.6). Tube lengths were measured (60 tubes per treatment; $n = 3$) with the image analysis system described above and with IPlab software (Applied Imaging International Ltd). For growth rate analysis, increases in individual pollen-tube lengths were measured at 5 min intervals for different treatments (30 min before, and up to 80 min after) by using IPlab software for image capture and analysis.

Detection of cytochrome *c* in pollen-tube extracts

For SI treatments, pollen was grown in liquid GM (ref. 3) for 1 h at 25 °C and then SI was induced as described above. To investigate the role of Ca^{2+} in cytochrome *c* release, samples of pollen tubes were treated with mastoparan (25 μM, 5 min). After treatment, pollen tubes were incubated for various durations and centrifuged at 33*g*; mitochondrial extraction buffer[21] was added to the pellet. Crude microsomal and cytosolic fractions were prepared as described in ref. 21. Equal concentrations of protein from both fractions were analysed by SDS–polyacrylamide-gel electrophoresis (SDS–PAGE) and western blotting[30]. Blots were probed with a 1:2,000 dilution of a monoclonal antibody raised against a peptide from cytochrome *c* (clone 7H8.2C12; BD Biosciences), probed with an anti-(mouse horseradish peroxidase) secondary antibody (Sigma) and detected by enhanced chemiluminescence (ECL; Amersham Biosciences). Quantification of changes in the amount of cytochrome *c* in cellular fractions was established by determining the intensity of the cytochrome *c* signal on western blots by densitometry with a Fluor-S multi-imager and Quantity One software (Bio-Rad). Readings (counts mm^{-2}) were background-subtracted.

Measurement of PARP-cleavage activity in pollen-tube extracts

Pollen was grown in liquid GM (ref. 3) and SI was induced as described above. Pollen tubes were collected by centrifugation, and HEPES buffer (50 mM HEPES pH 7.4, 10 mM NaCl, 0.1% CHAPS, 10 mM dithiothreitol, 1 mM EDTA, 10% glycerol) was added. Samples were snap-frozen in liquid N_2 and pollen protein extracts were prepared by grinding, centrifuged (13,200 *g* for 20 min at 4 °C) and the supernatant was tested for PARP-cleavage activity. Pollen cytosolic protein (30 μg) was incubated with 250 ng of bovine PARP (Biomol) at 37 °C for 15 min. Final sample buffer (5 × SDS)[30] was added; samples were boiled for 10 min and analysed by SDS–PAGE and western blotting with a 1:2,000 dilution of monoclonal antibody raised against PARP (clone F1-23, Biomol), which detects the PARP 24-kDa fragment. Controls consisted of bovine PARP incubated with HEPES buffer, and untreated pollen extracts. Blots were probed and developed, and quantification of the 24-kDa PARP cleavage product was performed by densitometry as described above. To investigate the role of Ca^{2+} in the PARP-cleavage activity, samples of pollen tubes were treated with mastoparan (25 μM, 30 min); or with $LaCl_3$ (500 mM, 30 min) before SI induction. The effect of caspase inhibitors on PARP cleavage was investigated by the incubation of 30 μg of pollen cytosolic extracts with 100 μM Ac-DEVD-CHO or Ac-YVAD-CHO for 10 min before the addition of bovine PARP.

Received 27 November 2003; accepted 2 April 2004; doi:10.1038/nature02540.

1. Franklin-Tong, V. E. & Franklin, F. C. H. Gametophytic self-incompatibility inhibits pollen tube growth using different mechanisms. *Trends Plant Sci.* **8,** 598–605 (2003).
2. Franklin-Tong, V. E., Ride, J. P., Read, N. D., Trewavas, A. J. & Franklin, F. C. H. The self-incompatibility response in *Papaver rhoeas* is mediated by cytosolic free calcium. *Plant J.* **4,** 163–177 (1993).
3. Rudd, J. J., Franklin, F. C. H., Lord, J. M. & Franklin-Tong, V. E. Increased phosphorylation of a 26-kD pollen protein is induced by the self-incompatibility response in *Papaver rhoeas*. *Plant Cell* **8,** 713–724 (1996).
4. Rudd, J. J., Osman, K., Franklin, F. C. H. & Franklin-Tong, V. E. Activation of a putative MAP kinase in pollen is stimulated by the self-incompatibility (SI) response. *FEBS Lett.* **547,** 223–227 (2003).
5. Geitmann, A., Snowman, B. N., Emons, A. M. C. & Franklin-Tong, V. E. Alterations in the actin cytoskeleton of pollen tubes are induced by the self-incompatibility reaction in *Papaver rhoeas*. *Plant Cell* **12,** 1239–1251 (2000).
6. Snowman, B. N., Kovar, D. R., Shevchenko, G., Franklin-Tong, V. E. & Staiger, C. J. Signal-mediated depolymerization of actin in pollen during the self-incompatibility response. *Plant Cell* **14,** 2613–2626 (2002).
7. Jordan, N. D., Franklin, F. C. H. & Franklin-Tong, V. E. Evidence for DNA fragmentation triggered in the self-incompatibility response in pollen of *Papaver rhoeas*. *Plant J.* **23,** 471–479 (2000).
8. Raff, M. Cell suicide for beginners. *Nature* **396,** 119–122 (1998).
9. Mittler, R. & Lam, E. Sacrifice in the face of foes: pathogen-induced programmed cell death in plants. *Trends Microbiol.* **4,** 10–15 (1996).
10. Fukuda, H. Programmed cell death of tracheary elements as a paradigm in plants. *Plant Mol. Biol.* **44,** 245–253 (2000).
11. Nagata, S., Nagase, H., Kawane, K., Mukae, N. & Fukuyama, H. Degradation of chromosomal DNA during apoptosis. *Cell Death Differ.* **10,** 108–116 (2003).
12. Scovassi, A. I. & Poirier, G. G. Poly(ADP-ribosylation) and apoptosis. *Mol. Cell. Biochem.* **199,** 125–137 (1999).
13. Salvesen, G. S. & Dixit, V. M. Caspase activation: the induced-proximity model. *Proc. Natl Acad. Sci. USA* **96,** 10964–10967 (1999).
14. Wolf, B. B., Schuler, M., Echeverri, F. & Green, D. R. Caspase-3 is the primary activator of apoptotic DNA fragmentation via DNA fragmentation factor-45/inhibitor of caspase-activated DNase inactivation. *J. Biol. Chem.* **274,** 30651–30656 (1999).
15. Wolf, B. B. & Green, D. R. Suicidal tendencies: Apoptotic cell death by caspase family proteinases. *J. Biol. Chem.* **274,** 20049–20052 (1999).
16. Garcia-Calvo, M. *et al.* Inhibition of human caspases by peptide-based and macromolecular inhibitors. *J. Biol. Chem.* **273,** 32608–32613 (1998).

17. Richael, C., Lincoln, J. E., Bostock, R. M. & Gilchrist, D. G. Caspase inhibitors reduce symptom development and limit bacterial proliferation in susceptible plant tissues. *Physiol. Mol. Plant Pathol.* **59,** 213–221 (2001).
18. Danon, A., Rotari, V. I., Gordon, A., Mailhac, N. & Gallois, P. Ultraviolet-C overexposure induces programmed cell death in *Arabidopsis*, which is mediated by caspase-like activities and which can be suppressed by caspase inhibitors, p35 and defender against apoptotic death. *J. Biol. Chem.* **279,** 779–787 (2004).
19. Woltering, E. J., van der Bent, A. & Hoeberichts, F. A. Do plant caspases exist? *Plant Physiol.* **130,** 1764–1769 (2002).
20. Adrain, C. & Martin, S. J. The mitochondrial apoptosome: a killer unleashed by the cytochrome seas. *Trends Biochem. Sci.* **26,** 390–397 (2001).
21. Balk, J., Leaver, C. J. & McCabe, P. F. Translocation of cytochrome *c* from the mitochondria to the cytosol occurs during heat induced programmed cell death in cucumber plants. *FEBS Lett.* **463,** 151–154 (1999).
22. Franklin-Tong, V. E., Drøbak, B. K., Allan, A. C., Watkins, P. A. C. & Trewavas, A. J. Growth of pollen tubes of *Papaver rhoeas* is regulated by a slow moving calcium wave propagated by inositol 1,4,5 trisphosphate. *Plant Cell* **8,** 1305–1321 (1996).
23. Babiychuk, E. *et al.* Higher plants possess two structurally different poly(ADP-ribose) polymerases. *Plant J.* **15,** 635–645 (1998).
24. Lepiniec, L., Babiychuk, E., Kushnir, S., Vanmontagu, M. & Inze, D. Characterization of an *Arabidopsis thaliana* cDNA homologue to animal poly(ADP-ribose) polymerase. *FEBS Lett.* **364,** 103–108 (1995).
25. Smith, S. The world according to PARP. *Trends Biochem. Sci.* **26,** 174–179 (2001).
26. Franklin-Tong, V. E., Holdaway-Clarke, T. L., Straatman, K. R., Kunkel, J. G. & Hepler, P. K. Involvement of extracellular calcium influx in the self-incompatibility response of *Papaver rhoeas*. *Plant J.* **29,** 333–345 (2002).
27. Dickinson, H. G. Simply a social disease? *Nature* **367,** 517–518 (1994).
28. Hodgkin, T., Lyon, G. D. & Dickinson, H. G. Recognition in flowering plants: a comparison of the *Brassica* self-incompatibility system and plant pathogen interactions. *New Phytol.* **100,** 557–569 (1988).
29. Kakeda, K. *et al.* Identification of residues in a hydrophilic loop of the *Papaver rhoeas* S protein that play a crucial role in recognition of incompatible pollen. *Plant Cell* **10,** 1723–1731 (1998).
30. Laemmli, U. K. Cleavage of structural proteins during the assembly of the head of bacteriophage T4. *Nature* **227,** 680–685 (1970).

Acknowledgements We thank C. Franklin and B. de Graaf for a critical reading of the manuscript. This work was funded by the BBSRC.

Competing interests statement The authors declare that they have no competing financial interests.

Correspondence and requests for materials should be addressed to V.E.F.T. (v.e.franklin-tong@bham.ac.uk).

Rab5 is a signalling GTPase involved in actin remodelling by receptor tyrosine kinases

Letizia Lanzetti[1], Andrea Palamidessi[1,2], Liliana Areces[1,2], Giorgio Scita[1,2] & Pier Paolo Di Fiore[1,2,3]

[1]*Istituto Europeo di Oncologia, Via Ripamonti 435, 20141 Milan, Italy*
[2]*IFOM, Istituto FIRC di Oncologia Molecolare, Via Adamello 16, 20139 Milan, Italy*
[3]*Dipartimento di Medicina, Chirurgia ed Odontoiatria, Universita' degli Studi di Milano, 20122 Milan, Italy*

Rab5 is a small GTPase involved in the control of intracellular trafficking, both at the level of receptor endocytosis and endosomal dynamics[1]. The finding that Rab5 can be activated by receptor tyrosine kinases (RTK)[2] raised the question of whether it also participates in effector pathways emanating from these receptors. Here we show that Rab5 is indispensable for a form of RTK-induced actin remodelling, called circular ruffling. Three independent signals, originating from Rab5, phosphatidylinositol-3-OH kinase and Rac, respectively, are simultaneously required for the induction of circular ruffles. Rab5 signals to the actin cytoskeleton through RN-tre, a previously identified Rab5-specific GTPase-activating protein (GAP)[3]. Here we demonstrate that RN-tre has the dual function of Rab5-GAP and Rab5 effector. We also show that RN-tre is critical for macropinocytosis, a process previously connected to the formation of circular ruffles[4,5]. Finally, RN-tre interacts with both F-actin and actinin-4, an F-actin bundling protein. We propose that RN-tre establishes a three-pronged connection with Rab5, F-actin and actinin-4. This may aid crosslinking of actin fibres into actin networks at the plasma membrane. Thus, we have shown that Rab5 is a signalling GTPase and have elucidated the major molecular elements of its downstream pathway.

Activation of RTKs leads to the formation of actin-based structures known as membrane ruffles, through the activation of the small GTPases Ras and Rac[5,6]. Ruffles are of at least two types: cell edge ruffles (lamellipodia) or dorsal surface ruffles (circular ruffles). Whereas lamellipodia are associated with cell motility/spreading, circular ruffles are involved in macropinocytosis and in three-dimensional migration[4,5,7]. Active RTKs induce both lamellipodia and circular ruffles[8]. A linear cascade, RTK → Ras → Rac seems sufficient for lamellipodia formation[9,10], whereas the molecular events leading to circular ruffles are less clear. Active mutants of Ras or Rac do not induce circular ruffles[9,10] (Supplementary Fig. 1), although an active form of Pak1, a Rac effector, does[11]. In addition, Ras and Rac are required for the induction of circular ruffles because dominant negative mutants of these proteins inhibit their formation[10,12]. Thus, concomitantly with the activation of Ras/Rac, additional RTK-triggered pathways may be required for circular ruffling.

Rab5 is a small GTPase required for the control of the endocytic route[1], and whose activity is regulated by guanine nucleotide exchange factors, such as Rabex5[13], and GAPs, such as RN-tre[3]. Rab5 has been linked to RTK- and Ras-activated signalling[2,14], and in addition, an active Rab5 mutant induced actin remodelling[15]. Thus, Rab5 is a candidate regulator in the pathway leading to circular ruffles. Indeed, a dominant negative Rab5 mutant ($Rab5^{S34N}$) inhibited the induction of circular ruffles by platelet derived growth factor (PDGF), whereas cell edge ruffles were unaffected (Fig. 1a). Overexpression of the Rab5-specific GAP RN-tre[3] also inhibited circular ruffles (Fig. 1a). Furthermore, Rab5 localized to PDGF-induced circular ruffles (Fig. 1b), similarly to Ras and Rac (Fig. 1c). Thus, the activity of Rab5 is required in a RTK-originated signalling pathway leading to circular ruffles. Notably, the effects of $Rab5^{S34N}$ and RN-tre were not the consequence of inhibiting endocytosis, which can be hypothesized based

Table 1 **Actin cytoskeleton remodelling activity of Rab5 in combination with various GTPases and effector proteins**

Transfection or PDGF treatment	Membrane ruffles (%)*	Circular ruffles (%)*
Ras^{V12}	+*(89‡)†	−(0)
$Rab5^{wt}$	−(2)	−(0)
$Rab5^{Q79L}$	−(3)	−(0)
Ras^{V12} + $Rab5^{wt}$	+(76‡)	+(23‡)
Ras^{V12} + $Rab5^{Q79L}$	+(88‡)	+(14‡)
$Ras^{V12,S35}$	−(2)	−(0)
$Ras^{V12,S35}$ + $Rab5^{wt}$	−(4)	−(0)
$Ras^{V12,C40}$	+(93‡)	−(0)
$Ras^{V12,C40}$ + $Rab5^{wt}$	+(90‡)	+(30‡)
$PI(3)K^{rCD2p110}$	+(76‡)	−(0)
$PI(3)K^{rCD2p110}$ + $Rab5^{wt}$	+(81‡)	+(22‡)
Rac^{Q61L}	+(88‡)	−(0)
Rac^{Q61L} + $Rab5^{wt}$	+(90‡)	−(0)
PDGF	+(91‡)	+(78‡)
PDGF + Rac^{N17}	−(3)	−(0)
Ras^{V12} + $Rab5^{wt}$ + Rac^{N17}	−(3)	−(0)
$PI(3)K^{rCD2p110}$ + $Rab5^{wt}$ + Rac^{N17}	−(2)	−(0)

*Actual images of selected experiments and further experimental controls are in Supplementary Figs 1 and 3. Unless otherwise specified (first column, PDGF), ruffles were scored under conditions of serum starvation. The phenotypes were detected (+) or not (−) in the transfected cells. Results are typical and represent at least three independent experiments, performed by transfection in MEFs.
†A quantification of the effects was performed in a single experiment, performed in triplicate in MEFs, by co-microinjection of the indicated plasmids. Phenotypes were scored by two observers. The numbers in parentheses (rounded up to the next higher integer) indicate the average number of cells displaying the phenotypes. At least 100 cells, in each triplicate, were counted.
‡Standard deviation was less than 20% of the mean. In the other samples, the number of events was too low for a meaningful statistical analysis.